

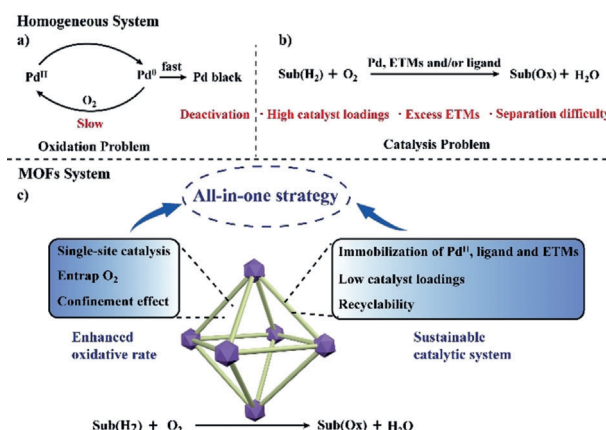


Palladium Catalysis for Aerobic Oxidation Systems Using Robust Metal–Organic Framework

Jiawei Li, Jianhua Liao, Yanwei Ren,* Chi Liu, Chenglong Yue, Jiaming Lu, and Huanfeng Jiang*

Abstract: Described here is a new and viable approach to achieve Pd catalysis for aerobic oxidation systems (AOSs) by circumventing problems associated with both the oxidation and the catalysis through an all-in-one strategy, employing a robust metal–organic framework (MOF). The rational assembly of a Pd^{II} catalyst, phenanthroline ligand, and Cu^{II} species (electron-transfer mediator) into a MOF facilitates the fast regeneration of the Pd^{II} active species, through an enhanced electron transfer from in situ generated Pd⁰ to Cu^{II}, and then Cu^I to O₂, trapped in the framework, thus leading to a 10 times higher turnover number than that of the homogeneous counterpart for Pd-catalyzed desulfitative oxidative coupling reactions. Moreover, the MOF catalyst can be reused five times without losing activity. This work provides the first exploration of using a MOF as a promising platform for the development of Pd catalysis for AOSs with high efficiency, low catalyst loading, and reusability.

Palladium-catalyzed aerobic oxidation reactions were the focus of synthetic chemistry in recent years owing to their crucial role for the synthesis of various valuable products.^[1] However, fast aggregation of the in situ generated Pd⁰ to Pd black (deactivation), compared to the slow electron transfer between Pd⁰ and molecular oxygen (O₂) constitutes the fundamental oxidation problem (Scheme 1 a).^[2] Extensive endeavors for solving this problem focused on the addition of electron-transfer mediators (ETMs) to carry the electron from Pd⁰ to O₂ along a low-energy pathway, thus boosting the reoxidation of Pd⁰ to Pd^{II}.^[3] Besides, considerable attention has been centered on the development of ancillary ligands to restrain the Pd⁰ aggregation.^[4] In spite of the significant progress offered by the above strategies (Scheme 1 b), these homogeneous Pd catalysis for aerobic oxidation systems (AOSs) often suffer from problems (such as high Pd^{II} loading, excess ETMs, and separation difficulties), which do not fulfill the requirements for atom-economy.^[5]



Scheme 1. a) Oxidation problem and b) catalysis problem in homogeneous Pd catalysis for AOSs. c) MOFs based Pd catalysis system using an all-in-one strategy.

Metal–organic framework (MOF) based heterogeneous catalysts have recently won a profound reputation because of their well-defined structural features.^[6] With precise knowledge of Pd-catalyzed aerobic oxidations, the highly tunable nature of MOFs enables the controllable immobilization of a Pd^{II} catalyst, ligand, and ETM. Meanwhile, the site-isolation nature and confinement effect of MOFs can stabilize the in situ generated Pd⁰ and enhance the electron-transfer efficiency. Moreover, MOFs can trap O₂ in the pores, and thereby create a local high-pressure O₂ atmosphere around the catalytic sites, thus further facilitating the efficient electron transfer between Pd⁰, the ETM, and O₂. Inspired by these merits, we envisioned MOFs serving as a promising platform for achieving advanced Pd-catalyzed AOSs through an all-in-one strategy (Scheme 1 c), thus solving the oxidation and catalysis problems of Pd-catalyzed aerobic oxidations in an efficient and sustainable manner. To the best of our knowledge, it has never been reported.

As a proof-of-concept, the Pd-catalyzed desulfitative oxidative coupling^[7] between arenesulfinic acid salts and an allylic alcohol was selected as a model reaction to verify the MOF-based catalytic system because this reaction possesses the representative oxidation and catalysis problems of Pd-catalyzed AOSs. For example, the homogeneous system needs a high loading of Pd(TFA)₂ (10 mol %) as the catalyst, phenanthroline (phen; 20 mol %) as the ligand, and a stoichiometric amount of Cu(TFA)₂ as the ETM to achieve high reactivity. Herein, we utilize a phen-containing linker, 1,10-phenanthroline-3,8-dicarboxylic acid (PDC), as a difunctional ligand to construct a zirconium-based MOF (UiO series),

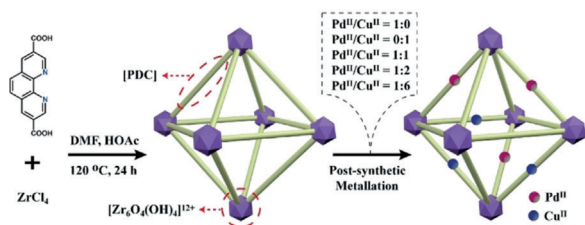
[*] Dr. J. Li, Dr. Y. Ren, C. Liu, C. Yue, J. Lu, Prof. Dr. H. Jiang
Key Laboratory of Functional Molecular Engineering of Guangdong Province, School of Chemistry and Chemical Engineering, South China University of Technology
Guangzhou 510641 (P. R. China)
E-mail: renyw@scut.edu.cn
jjanghf@scut.edu.cn

Dr. J. Liao
School of Pharmaceutical Sciences, Gannan Medical University
Ganzhou 341000 (P. R. China)

Supporting information and the ORCID identification number(s) for the author(s) of this article can be found under:
<https://doi.org/10.1002/anie.201909661>.

which can be metallized to achieve MOF-based Pd catalysis of AOSs. The porous, stable, and tunable UiO MOFs have been regarded as excellent carriers for heterogeneous catalysis.^[8]

As shown in Scheme 2, solvothermal reaction of $ZrCl_4$ and PDC afforded block nanoparticles (average size of about 30 nm), as confirmed by scanning-electron microscopy (SEM) and transmission-electron microscopy (TEM) images (see Figure S6 in the Supporting Information), termed UiO-67-



Scheme 2. Syntheses of metallized UiO-67-phen.

phen. The purity and crystallinity of UiO-67-phen were confirmed by its PXRD pattern, which matches well with that of UiO-67^[9] (Figure 1 a), suggesting they have the same topological structure. UiO-67, comprising 12 connected $[Zr_6O_4(OH)_4]^{12+}$ clusters and biphenyl-4,4'-dicarboxylate (BPDC) ligands, contains two types of cages: an octahedral cage and a tetrahedral cage, both of which are accessible by equilateral triangle windows with side lengths of about 1.2 nm.^[9] Because of the same molecular length of PDC and BPDC, the pore structure of UiO-67-phen should be similar to that of UiO-67. The Brunauer-Emmett-Teller (BET) area of UiO-67-phen is calculated to be $1845 \text{ cm}^3 \text{ g}^{-1}$ with a pore width distribution centered at 1.1 nm according to the N_2 adsorption isotherm at 77 K (Figures 1 b,c). Thermal gravimetric analysis (TGA) reveals a thermal stability for UiO-67-phen of up to 450°C (see Figure S2), guaranteeing its usage in high-temperature reactions. The metallized analogues, UiO-67-phen-Pd/Cu(*x*:*y*) [*x*:*y* = 1:0, 1:1, 1:2, 1:6, 0:1], were post-

synthesized by varying the initial $Pd(TFA)_2/Cu(TFA)_2$ ratios. The inductively coupled plasma mass spectrometry (ICP-MS) analyses showed the molar ratios of Zr/Pd/Cu in the metallized MOFs to be 6:2:0, 6:1.4:1.3, 6:1:2, 6:0.4:2.4, and 6:0:3.7, respectively. PXRD patterns of these metallized MOFs indicate the maintenance of their structural integrity (Figure 1 a; see Figure S1). The reduced N_2 adsorbed quantities, BET areas, and pore sizes of the metallized MOFs can be explained by the embedding of Pd and Cu salts into the framework (Figures 1 b,c). SEM and elemental mapping images display uniform distribution of Zr, Pd, and Cu over these metallized MOFs (see Figure S7).

To verify the valence state of the Pd and Cu species, and their coordination modes in the metallized MOFs, X-ray photoelectron spectroscopy (XPS) analyses were performed (Figures 1 d–f). The characteristic peaks of binding energies (BEs) of Pd $3d_{5/2}$ at 338 eV and Pd $3d_{3/2}$ at 344 eV indicate the oxidation state of Pd is +2.^[10] The divalent Cu state can be inferred by the peaks of BEs located at 934 and 952 eV, corresponding to Cu $2p_{3/2}$ and Cu $2p_{1/2}$, respectively, as well as two typical satellite peaks at 940 and 945 eV.^[11] The BE of N 1s in UiO-67-phen is 399 eV, which is attributed to the nitrogen in phen, and is similar to that of 2,2'-bipyridine based UiO-67-bpy.^[12] In contrast, there are two N 1s peaks of BEs in UiO-67-phen-Pd/Cu(1:0) and UiO-67-phen-Pd/Cu(0:1), signifying that the nitrogen atoms present two types of coordination environments. One peak is analogous to UiO-67-phen, and the other shifts toward a higher BE because of a decrease in the electron density of the N atom by the coordination between the N atoms in phen and Pd^{II} (or Cu^{II}) ions. For UiO-67-phen-Pd/Cu(1:2), there are three types of N 1s peaks located at 400.5, 400 and 399 eV, implying the coexistence of free phen, Pd^{II}-phen, and Cu^{II}-phen species. These results clearly confirm the successful insertion of Pd^{II} and Cu^{II} into UiO-67-phen, wherein the two cations coordinate to phen with TFA^- as a counterion as determined by ^{19}F NMR data (Figure S8).

To explore the catalytic performance of the metallized UiO-67-phen, the desulfative oxidative coupling reaction

between sodium benzenesulfinate (**1a**) and but-3-en-2-ol (**2a**) was selected. It turned out the reaction proceeded smoothly in the presence of UiO-67-phen-Pd/Cu(1:6) at optimal reaction conditions, giving the desired β -aryl ketone in excellent yield (Table 1, entry 8). In contrast, when reducing the amount of Cu^{II} from 100 to 60 mol% in the homogeneous system, sharp decreases in yield could be observed (entry 2). This difference between homogeneous and MOF systems became more remarkable as the amount of Cu^{II} further reduced to 20 mol%

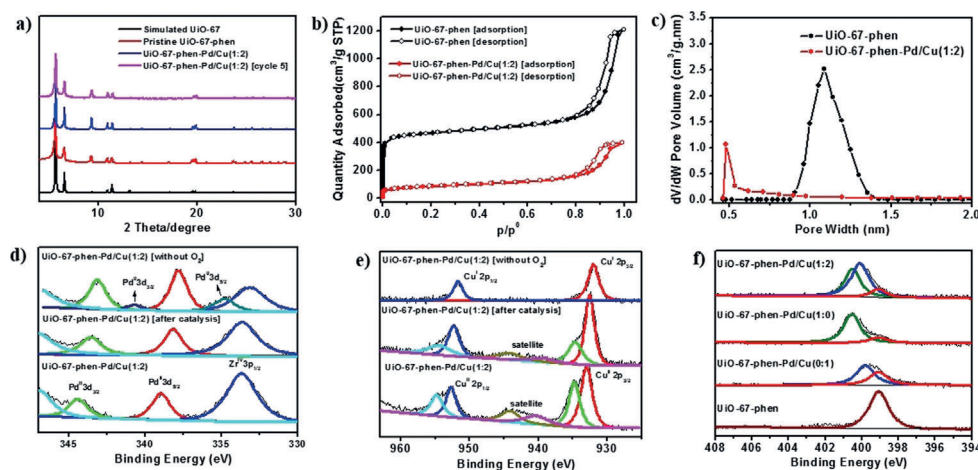
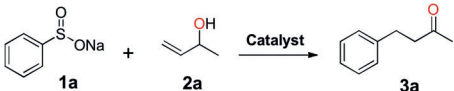


Figure 1. a) PXRD patterns. b) N_2 adsorption and desorption isotherms. c) Pore size distributions. d) XPS spectra of the Pd 3d region. e) XPS spectra of the Cu 2p region. f) XPS spectra of the N 1s for UiO-67-phen and metallized UiO-67-phen, respectively.

Table 1: Comparison of homogeneous and MOFs systems for the desulfative oxidative coupling reaction between **1a** and **2a**.^[a]


Entry	Catalytic system	Yield[%] ^[b]	TON ^[c]
<i>Homogeneous system</i> ^[d]			
1 ^[e]	Pd(TFA) ₂ [10 mol%]/Cu(TFA) ₂ [100 mol%]	80	8
2	Pd(TFA) ₂ [10 mol%]/Cu(TFA) ₂ [60 mol%]	52	5.2
3	Pd(TFA) ₂ [10 mol%]/Cu(TFA) ₂ [20 mol%]	20	2
4	Pd(TFA) ₂ [10 mol%]/Cu(TFA) ₂ [10 mol%]	11	1.1
5	Pd(TFA) ₂ [10 mol%]	6	0.6
6	Pd(TFA) ₂ [1 mol%]/Cu(TFA) ₂ [2 mol%]	4	4
<i>MOFs system</i>			
7	UiO-67-phen (or no catalyst)	–	–
8	UiO-67-phen-Pd/Cu(1:6) [10 mol% Pd]	87	8.7
9	UiO-67-phen-Pd/Cu(1:2) [10 mol% Pd]	88	8.8
10	UiO-67-phen-Pd/Cu(1:1) [10 mol% Pd]	71	7.1
11	UiO-67-phen-Pd/Cu(1:0) [10 mol% Pd]	52	5.2
12	UiO-67-phen-Pd/Cu(0:1) [20 mol% Cu]	–	–
13 ^[e]	UiO-67-phen-Pd/Cu(1:2) [10 mol% Pd]	38	3.8
14	UiO-67-phen-Pd/Cu(1:2) [5 mol% Pd]	86	17.2
15	UiO-67-phen-Pd/Cu(1:2) [1 mol% Pd]	89	89
16	UiO-67-phen-Pd/Cu(1:2) [0.2 mol% Pd]	46	230

[a] The reaction conditions were: **1a** (0.5 mmol), **2a** (2 mmol), O₂ (1 atm), 1,4-dioxane (3 mL), 100 °C and 20 h. [b] Determined by GC-MS with *n*-dodecane as internal standard. [c] TON (turnover number): moles of product per mole of catalyst used. [d] For homogeneous system, 4,7-dimethyl-1,10-phenanthroline (20 mol%) was added. [e] Under anaerobic conditions.

(entries 3 and 9). As stoichiometric quantities or an excess amount of the ETM are usually required to regenerate Pd^{II} in homogeneous systems,^[3b] the decreased ETM loading should reduce the interaction between Pd⁰ and the ETM in solution, leading to an unfavorable electron transfer and thus a dramatic decrease in activity. For the MOF system, the aggregation of the in situ generated Pd⁰ should be prohibited by the MOFs site isolation, and the fast electron transfer from Pd⁰ to adjacent Cu²⁺ atoms should be achieved given their close positioning within the confined pores of UiO-67-phen, even at lower Cu²⁺ loadings. Although further reduction in the amount of Cu^{II} to 10 mol% leads to slightly decreased yield (entry 10), the MOF still outperforms the homogeneous system.

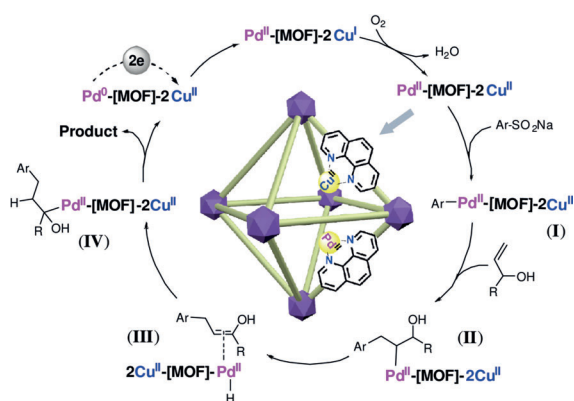
When O₂ (1 atm) was utilized as the sole oxidant, UiO-67-phen-Pd/Cu(1:0) still gave a moderate yield (Table 1, entry 11), while only 6% yield could be observed for the homogeneous system (entry 5). These findings distinctly suggest a different behavior of O₂ within MOF relative to the homogeneous system. The entrapment of O₂ within UiO-67-phen-Pd/Cu(1:0) (see Figure S5) may form a local high-pressure O₂ atmosphere within the framework, thus enhancing the electron-transfer efficiency between O₂ and Pd⁰, as high-pressure O₂ has been evidenced to increase the reoxidation rate of Pd⁰ in homogeneous systems.^[13] Additionally, when UiO-67-phen-Pd/Cu(1:2) was utilized under anaerobic conditions, an obviously reduced yield was observed (entry 13). XPS investigation of this recovered catalyst was

conducted to prove the change of valence state of Cu and Pd species (Figures 1 d,e). The absence of two satellite peaks at the copper 2p level and the presence of two new peaks (334 and 341 eV) at the palladium 3d level demonstrate that almost all Cu^{II} has been converted into Cu^I [11] and that a number of Pd species were in the reduced form.^[14]

Decreasing the loading of UiO-67-phen-Pd/Cu(1:2) to 1 mol% (based on Pd) could also catalyze the reaction without compromising the reactivity, leading to a 10 times higher TON and 50 times less Cu consumption than homogeneous counterparts (Table 1, entries 6 and 15). Further lowering the catalyst loading to 0.2 mol% leads to a TON of 230 (entry 16). The above findings indicate that the Pd^{II} and ETM species in the framework display prominent activities, especially at low catalyst/substrate ratio, probably as a result of the confinement effect of the framework and/or high surface utilization of MOF nanoparticles. Note that UiO-67-phen-Pd/Cu(1:2) could be reused for at least five cycles without apparent loss of activity (see Figure S10). ICP-MS of the reaction filtrate showed negligible leaking of Pd^{II} and Cu^{II} ions into the solution, confirming the heterogeneous nature of this reaction. The PXRD pattern and N₂ adsorption isotherm of the recovered catalyst revealed that the porosity and crystallinity were maintained after the catalysis (Figure 1 a; see Figure S3). XPS data imply that the oxidation states of Pd and Cu remain at +2 after the catalysis (Figures 1 d,e), and the TEM image showed no detectable Pd⁰ nanoparticles over the framework (see Figure S9).

Next, the general applicability was examined, and a series of different sodium arylsulfonates bearing electron-donating and electron-withdrawing groups at the *para*-position were found to be suitable substrates, producing the corresponding β-aryl ketones in good to excellent yields (see Table S1, **3b–e**). Phenyl-substituted allyl alcohol was well tolerated to this reaction, giving the desired product in moderate yield (see Table S1, **3f**). An aliphatic allyl alcohol with an elongated chain could also be converted into the corresponding product in excellent yield (see Table S1, **3g**). Besides, allyl primary alcohol was found to be active, resulting in the formation of β-aryl aldehyde in good yield (see Table S1, **3h**).

Based on above results and previous reports,^[7] we propose a plausible mechanism of the Pd-catalyzed oxidative coupling reaction within UiO-67-phen-Pd/Cu(1:2) (Scheme 3). The aromatic sulfinic sodium is firstly coordinated to Pd^{II} in the MOF with the extrusion of SO₂. Then, the Heck-type insertion of the allyl alcohol to the arylpalladium complex **I** occurs, affording the σ-alkylpalladium complex **II**. The selective β-hydride elimination of **II** gives the enol complex **III**, which subsequently changes to **IV** with the transfer of hydrogen to the α-carbon atom by spontaneous insertion of 2Cu^{II}-[MOF]-Pd^{III}H. Either elimination of **IV** from the α-OH or an anion-mediated reductive elimination is possible to afford the final product, accompanied by the generation of a Pd⁰ species. Different from a homogeneous system, the efficient catalyst cycle was accomplished through the fast electron transfer within the MOF. Initially, the in situ generated Pd⁰ is prohibited from fast aggregation by the MOFs catalytic site isolation. Subsequently, two electrons transfer immediately from the generated Pd⁰ to adjacent Cu^{II}



Scheme 3. Proposed mechanism.

ions, leading to the regeneration of Pd^{II} active species and the reduction of Cu^{II} to Cu^I. Finally, Cu^I can be reoxidized to Cu^{II} by the local high-pressure O₂ trapped within the UiO-67-phen, thereby realizing the catalytic cycle. In general, there are three electron-transport mechanisms in MOFs: a) through-bond conduction, b) through-space conduction (such as π - π stacking), and c) hopping transport.^[15] According to the close position of Pd and Cu species coordinated on phen in UiO-67-phen-Pd/Cu(1:2), the redox hopping is likely the mechanism of electron transfer.

In summary, through an all-in-one strategy, we have developed an advanced Pd catalysis AOS by controllably immobilizing Pd^{II} and Cu^{II} species onto the framework of a UiO MOF. This MOF-based catalyst exhibits markedly increased TONs and largely reduced ETM consumption compared to its homogeneous counterparts for Pd-catalyzed desulfative oxidative coupling reaction. Preorganization of Pd^{II} and Cu^{II}, as well as the capacity of entrapped O₂ within the MOF facilitate efficient electron transfer and speed up the catalytic cycle, and the site isolation of Pd^{II} and heterogeneous nature of the MOFs increase the catalyst reusability, therefore subtly resolving the oxidation and catalysis problems, respectively. This work demonstrates, for the first time, the ability to merge a Pd^{II} catalyst, a ligand, and ETM into one single MOF support to boost Pd-catalyzed aerobic oxidation activity, and highlights a new strategy to achieve advanced Pd catalysis for AOSs in an efficient and sustainable manner.

Experimental Section

The experimental details included in the Supporting Information.

Acknowledgements

We are grateful for the financial support from the National Key Research and Development Program of China (2016YFA0602900) and the National Natural Science Foundation of China (21420102003).

Conflict of interest

The authors declare no conflict of interest.

Keywords: aerobic oxidation · copper · heterogeneous catalysis · metal–organic framework · palladium

- [1] a) S. S. Stahl, *Science* **2005**, *309*, 1824–1826; b) W. Q. Wu, H. F. Jiang, *Acc. Chem. Res.* **2012**, *45*, 1736–1748; c) B. Yang, Y. Qiu, J. E. Bäckvall, *Acc. Chem. Res.* **2018**, *51*, 1520–1531; d) G. Yin, X. Mu, G. Liu, *Acc. Chem. Res.* **2016**, *49*, 2413–2423; e) M. S. Sigman, D. R. Jensen, *Acc. Chem. Res.* **2006**, *39*, 221–229; f) X. F. Wu, H. Neumann, M. Beller, *ChemSusChem* **2013**, *6*, 229–241.
- [2] a) A. N. Campbell, S. S. Stahl, *Acc. Chem. Res.* **2012**, *45*, 851–863; b) Z. Shi, C. Zhang, C. Tang, N. Jiao, *Chem. Soc. Rev.* **2012**, *41*, 3381–3430.
- [3] a) J. Liu, A. Ricke, B. Yang, J. E. Bäckvall, *Angew. Chem. Int. Ed.* **2018**, *57*, 16842–16846; *Angew. Chem.* **2018**, *130*, 17084–17088; b) J. Pira, J. E. Bäckvall, *Angew. Chem. Int. Ed.* **2008**, *47*, 3506–3523; *Angew. Chem.* **2008**, *120*, 3558–3576.
- [4] a) L. Jin, A. Lei, *Sci. Chin.-Chem.* **2012**, *55*, 2027–2035; b) D. Wang, A. B. Weinstein, P. B. White, S. S. Stahl, *Chem. Rev.* **2018**, *118*, 2636–2679; c) W. Zhang, P. Chen, G. Liu, *Angew. Chem. Int. Ed.* **2017**, *56*, 5336–5340; *Angew. Chem.* **2017**, *129*, 5420–5424.
- [5] M. O. Simon, C. Li, *Chem. Soc. Rev.* **2012**, *41*, 1415–1427.
- [6] a) Y. Bai, Y. Dou, L. H. Xie, W. Rutledge, J. R. Li, H. C. Zhou, *Chem. Soc. Rev.* **2016**, *45*, 2327–2367; b) T. Drake, P. Ji, W. Lin, *Acc. Chem. Res.* **2018**, *51*, 2129–2138; c) L. Jiao, H.-L. Jiang, *Chem* **2019**, *5*, 786–804; d) L. Jiao, Y. Wang, H. L. Jiang, Q. Xu, *Adv. Mater.* **2018**, *30*, 1703663.
- [7] J. Liao, Z. Zhang, X. Tang, W. Wu, W. Guo, H. Jiang, *J. Org. Chem.* **2015**, *80*, 8903–8909.
- [8] a) J. S. Qin, S. Yuan, C. Lollar, J. Pang, A. Alsalmeh, H. C. Zhou, *Chem. Commun.* **2018**, *54*, 4231–4249; b) M. Rimoldi, A. J. Howarth, M. R. DeStefano, L. Lin, S. Goswami, P. Li, J. T. Hupp, O. K. Farha, *ACS Catal.* **2017**, *7*, 997–1014.
- [9] J. H. Cavka, S. Jakobsen, U. Olsbye, N. Guillou, C. Lamberti, S. Bordiga, K. P. Lillerud, *J. Am. Chem. Soc.* **2008**, *130*, 13850–13851.
- [10] S. Y. Ding, J. Gao, Q. Wang, Y. Zhang, W. G. Song, C. Y. Su, W. Wang, *J. Am. Chem. Soc.* **2011**, *133*, 19816–19822.
- [11] M. C. Biesinger, L. W. M. Lau, A. R. Gerson, R. S. C. Smart, *Appl. Surf. Sci.* **2010**, *257*, 887–898.
- [12] B. Li, Z. Ju, M. Zhou, K. Su, D. Yuan, *Angew. Chem. Int. Ed.* **2019**, *58*, 7687–7691; *Angew. Chem.* **2019**, *131*, 7769–7773.
- [13] a) M. Hu, W. Wu, H. Jiang, *ChemSusChem* **2019**, *12*, 2911–2935; b) T. Mitsudome, T. Umetani, N. Nosaka, K. Mori, T. Mizugaki, K. Ebitani, K. Kaneda, *Angew. Chem. Int. Ed.* **2006**, *45*, 481–485; *Angew. Chem.* **2006**, *118*, 495–499.
- [14] B. Z. Yuan, Y. Y. Pan, Y. W. Li, B. L. Yin, H. F. Jiang, *Angew. Chem. Int. Ed.* **2010**, *49*, 4054–4058; *Angew. Chem.* **2010**, *122*, 4148–4152.
- [15] a) F. Rouhani, F. Rafizadeh-Masuleh, A. Morsali, *J. Am. Chem. Soc.* **2019**, *141*, 11173–11182; b) L. Sun, M. G. Campbell, M. Dinca, *Angew. Chem. Int. Ed.* **2016**, *55*, 3566–3579; *Angew. Chem.* **2016**, *128*, 3628–3642.

Manuscript received: August 3, 2019

Accepted manuscript online: September 5, 2019

Version of record online: ■■■■■■

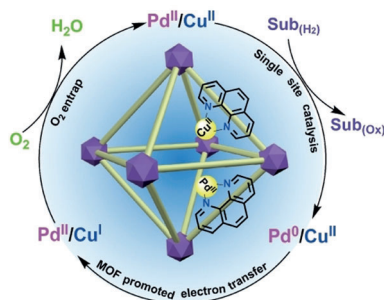
Communications



Heterogeneous Catalysis

J. Li, J. Liao, Y. Ren,* C. Liu, C. Yue, J. Lu,
H. Jiang* ————— ■■■■—■■■■

Palladium Catalysis for Aerobic Oxidation
Systems Using Robust Metal–Organic
Framework



All-in-one: Immobilizing Pd^{II} and Cu^I species into a robust metal–organic framework (MOF) facilitates the Pd catalysis for an aerobic oxidation system, a desulfurative oxidative coupling reaction, with high efficiency, low catalyst loading, and reusability. These results demonstrate the ability to merge a Pd^{II} catalyst, a ligand, and an electron-transfer mediator into a single MOF to boost activity in an efficient and sustainable manner.